

# Lawrence Berkeley National Laboratory

## Recent Work

### Title

A MOLECULAR DYNAMICS STUDY OF THE REACTION:  $\text{H}_2 + \text{OH} \rightarrow \text{H}_2\text{O} + \text{H}$

### Permalink

<https://escholarship.org/uc/item/2w2355k3>

### Authors

Rashed, O.  
Brown, N.J.

### Publication Date

1984-10-01



# Lawrence Berkeley Laboratory

UNIVERSITY OF CALIFORNIA

RECEIVED  
LAWRENCE  
BERKELEY LABORATORY  
NOV 1 1984  
LIBRARY AND  
DOCUMENTS SECTION

## APPLIED SCIENCE DIVISION

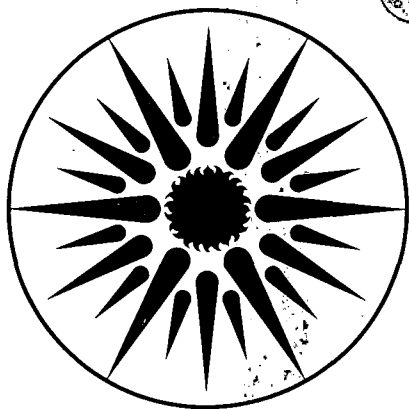
Presented at the Western States Section/The  
Combustion Institute 1984 Fall Meeting,  
Stanford University, Stanford, CA,  
October 22-23, 1984

A MOLECULAR DYNAMICS STUDY OF THE REACTION:  
 $H_2 + OH \rightarrow H_2O + H$

O. Rashed and N.J. Brown

October 1984

TWO-WEEK LOAN COPY  
This is a Library Circulating Copy  
which may be borrowed for two weeks



APPLIED SCIENCE  
DIVISION

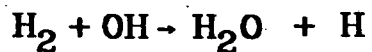
LBL-18531  
c.2

## **DISCLAIMER**

This document was prepared as an account of work sponsored by the United States Government. While this document is believed to contain correct information, neither the United States Government nor any agency thereof, nor the Regents of the University of California, nor any of their employees, makes any warranty, express or implied, or assumes any legal responsibility for the accuracy, completeness, or usefulness of any information, apparatus, product, or process disclosed, or represents that its use would not infringe privately owned rights. Reference herein to any specific commercial product, process, or service by its trade name, trademark, manufacturer, or otherwise, does not necessarily constitute or imply its endorsement, recommendation, or favoring by the United States Government or any agency thereof, or the Regents of the University of California. The views and opinions of authors expressed herein do not necessarily state or reflect those of the United States Government or any agency thereof or the Regents of the University of California.

To be presented at the Western States Section/  
The Combustion Institute 1984 Fall Meeting, at  
Stanford University, Stanford, CA, October 22-23, 1984.  
Paper No. 84-93.

**A Molecular Dynamics Study of the Reaction:**



O. Rashed and N. J. Brown  
Applied Science Division  
Lawrence Berkeley Laboratory  
University of California  
Berkeley, California 94720

This work was supported by the Director, Office of Energy Research, Office of  
Basic Energy Sciences, Chemical Sciences Division of the U.S. Department of  
Energy under Contract No. DE-AC-03-765F00098.

## ABSTRACT

Classical trajectory calculations have been performed to determine the influence of translational temperature,  $H_2$  vibrational energy,  $H_2$  rotational energy, OH vibrational energy, and OH rotational energy on the reaction,  $H_2 + OH \rightarrow H_2O + H$ . The potential energy surface was a modification of the Schatz-Elgersma analytical fit to the Walsh-Dunning surface. Reactivity increases with translational temperature, and is most strongly influenced by it. Rotational excitation of either or both molecules suppresses reactivity. Vibrational excitation of  $H_2$  enhances reactivity, and vibrational excitation of OH has no effect. A thermal rate coefficient was computed for the reaction at 1200 and 2000 K. The computed value compares favorably with the experiment at 2000 K, while the agreement at 1200 K is less satisfactory. The agreement between theory and experiment at both temperatures indicates that the potential surface is a reasonable representation of the HHOH potential energy surface.

## I. INTRODUCTION

Bimolecular radical shuffling reactions in the gas phase represent an important class of elementary processes in complex systems, particularly combustion. The bimolecular reaction between  $H_2$  and OH which produces  $H_2O$  and H, is extremely important in combustion systems. In hydrogen/oxygen flame systems, this reaction appears to be the principal source of water production at temperatures above 700 K to temperatures prior to the onset of partial equilibrium. It is also the main source of water<sup>2</sup> in typical hydrocarbon-air flames at atmospheric pressure. Due to its importance, the  $H_2 + OH$  reaction has been the object of extensive theoretical and experimental study.

Walsh and Dunning<sup>3</sup> computed barrier heights and transition state geometries for HHOH using large scale POL-CI wave functions. Dunning et al.,<sup>4</sup> discuss the characteristics of the surface and indicate that the agreement between the computed vibrationally adiabatic threshold (5.9 kcal/mol) and experimentally derived values of the activation energy (4-6 kcal/mol) is quite reasonable. Schatz and Elgersma<sup>5</sup> fitted the Walsh-Dunning surface to an analytical form and performed a molecular dynamics calculation to determine the product vibrational states for four values of the translational energy. In a second study, Schatz and Elgersma<sup>6</sup> examined the rotational, angular, and projection distributions of products in the  $H_2 + OH$  reaction. In a later study, Schatz<sup>7</sup> performed a quasiclassical trajectory study to determine the effects of reagent vibrational excitation on reactivity. Classical transition state calculations were also performed by Schatz and Walsh,<sup>8</sup> and Isaacson and Truhlar<sup>9</sup> computed rate coefficients for the reaction using variational transition state theory and semiclassical vibrationally adiabatic transition theory. More recently Brown and Edlin<sup>10</sup> performed transition state theory calculations on the  $H_2 + OH$  reaction taking full account of angular momentum conservation and with tunneling corrections. Rate coefficients were also computed for all possible isotopes achieved by substituting one or two H atoms with D.

There has been a corresponding experimental effort placed upon determining the  $H_2 + OH$  rate coefficient over a wide range of temperatures, and to determine factors influencing reactivity. Three reviews<sup>2,11,12</sup> of the kinetics of this reaction are available. Brown et al.,<sup>1</sup> determined a rate coefficient for the reaction in low pressure hydrogen/oxygen flame studies, and Ravishankara et al.<sup>13</sup>, measured the thermal rate of OH with  $H_2$  and  $D_2$  from 250 to 1050 K using a flash photolysis-resonance fluorescence technique. Spencer et al.,<sup>14</sup> and Light and Matsumoto<sup>15</sup> investigated the effect of vibrationally excited OH on the reaction. Zellner and Steinert<sup>16-17</sup> have recently measured the effect of vibrationally excited  $H_2$  on the rate at 298 K.

In our own study, which is a quasiclassical molecular dynamics study of the  $H_2 + OH \rightarrow H_2O + H$  reaction with a modified potential energy surface, we have attempted to understand the role the system's initial energy distribution plays in influencing reactivity. We have also computed a series of reaction cross sections necessary to determine the thermal rate coefficient at 1200 and 2000 K. We have placed special emphasis on determining the effect of reagent rotation on reactivity, and have also examined the influence of reagent vibrational energy and translational temperature. Energy transfer in non-reactive and reactive collisions will be the subject of another paper and will not be discussed in detail here.

## II. MATHEMATICAL MODEL

The method of quasi-classical dynamics discussed by many investigators are used in this study. The particular formalism used here incorporates three basic approximations: 1) the use of the Rashed-Brown modification to the Schatz-Elgersma analytical fit to the Walsh-Dunning potential surface, 2) the treatment of the dynamics with classical mechanics, and 3) the use of Monte Carlo averaging techniques to sample the entire phase space of the  $H_2 + OH$  system.

## A. The Potential Energy Surface

The potential energy surface used in this study is a modified form of the Schatz-Elgersma<sup>5</sup> (S-E) analytical representation of the Walsh-Dunning *ab initio* potential energy surface. Walsh and Dunning used large scale POL-CI wave functions to compute barrier heights and transition state geometries. Several *ab initio* points were computed in the vicinity of the saddle point region to determine the transition state geometry, and a few were computed in the asymptotic regions of configuration space. The S-E empirical fit to the Walsh-Dunning points expresses the potential as a function of the six distances between the atoms. The analytical form adopted consists of six, two-body terms, which are Morse and LEPS functions, two, three-body terms, which are quadratic Sorbie-Murrell-like terms<sup>18</sup> giving  $H_2O$  the correct quadratic force field,<sup>19</sup> and a four body correction term. Figure 1 is a schematic diagram of the HHOH system illustrating the pertinent distances. The potential energy surface is thus written in the following form:

$$\begin{aligned} V = & V_M(R_6) + V_M'(R_4) + V_M'(R_2) \\ & + V_{LEPS}(R_5, R_3, R_1) \\ & + V_{H_2O}(R_6, R_5, R_4) + V_{H_2O}(R_6, R_3, R_2) \\ & + V_4(R_5, R_3, R_4, R_2) \end{aligned} \quad (2.1)$$

where the distances are identified in Fig. 1, and  $V_M$  and  $V_M'$  are Morse terms,  $V_{LEPS}$  is a LEPS potential,  $V_{H_2O}$  is a Sorbie-Murrell-like three body term, and  $V_4$  is the four body term. The exact form of these terms and the appropriate constants are given by Schatz and Elgersma.<sup>5</sup> This functional form treats  $H_2$  and  $H_3$  as identical, but treats  $H_1$  differently. The saddle point barrier height and zero point energy are in good agreement with the *ab initio* results, but the agreement with regard to saddle point geometry and frequencies is less satisfactory. Schatz and Elgersma discuss the difficulty in fitting the surface away from the saddle point due to the lack of *ab initio* points in these regions and inflexibility in the



functional form. They mention the existence of small bumps in the surface of approximately 2.3 kcal/mol magnitude. We discovered spurious well of magnitude 2-3 kcal/mol, in the asymptotic region of the surface which gave rise to anomalously long-lived trajectories at values of translational energy important in our calculations, namely, for trajectories with translational energy less than 5 kcal/mol.

Careful analysis of the various terms in the potential revealed that the Morse terms describing the interaction between  $H_1$  and  $H_2$  and  $H_1$  and  $H_3$ , were not approaching zero quickly enough. These contribute negative energy to the potential and result in the existence of wells in the asymptotic region. The most satisfactory method of correcting this undesirable behavior was to increase the value of  $\beta$  in the Morse function thus making the function approach zero more quickly. This was accomplished by analytically continuing the S-E Morse function at distances  $d$ , with  $5.2 < d < 5.5$  bohr with a cubic spline function, and then increasing the value of  $\beta$ , as shown in the following equations. The potential is the SE potential for  $R_4 < 5.2$  and  $R_2 < 5.2$ . The terms  $V_M'(R_2)$  and  $V_M'(R_4)$  are each replaced by a cubic spline for either  $5.2 < R_2 < 5.5$  or  $5.2 < R_4 < 5.5$  with

$$V_{spline} = a + (R-5.2)(b+R-5.5)(c+(R-5.2)d) \quad (2.2)$$

and

$$\begin{aligned} a &= f_1 \\ b &= (f_2 - f_1) / (5.5 - 5.2) \\ c &= (f_3 - b) / (5.2 - 5.5) \\ d &= [(f_4 - b) / (5.5 - 5.2) - b] / (5.5 - 5.2) \end{aligned} \quad (2.3)$$

with

$$\begin{aligned}f_1 &= De(1 - e^{-\beta(5.2 - R_0)})^2 \\f_2 &= De(1 - e^{-\beta'(5.5 - R_0)})^2 \\f_3 &= 2\beta De(1 - e^{-\beta(5.2 - R_0)})e^{-\beta(5.2 - R_0)} \\f_4 &= 2\beta' De(1 - e^{-\beta'(5.5 - R_0)})e^{-\beta'(5.2 - R_0)}\end{aligned}\tag{2.4}$$

and with

$$\begin{aligned}\beta &= .924 \text{ bohr}^{-1} \\De &= .02757 \text{ hartree} \\Re &= 2.908 \text{ bohr} \\\beta' &= 1.48 \text{ bohr}^{-1}\end{aligned}\tag{2.5}$$

for  $R_2 > 5.5$  bohr the term  $V_M'(R_2)$  is evaluated with the new value the Morse constant,  $\beta' = 1.48 \text{ bohr}^{-1}$ , and for  $R_4 > 5.5$  bohr,  $V_M'(R_4)$  is also evaluated with  $\beta'$ .

This modification to the S-E potential allowed one to achieve the proper asymptotic behavior through removal of the spurious wells at large internuclear separations. The character of the potential near the saddle point geometry was retained since the analytical fit was particularly good in this region due to the high density of *ab initio* points.

Figure 2 and 3 are plots of S-E and R-B potential energy as a function of the center-of-mass separation of the  $H_2$  and OH molecules. The energy for the two surfaces was computed along trajectories with identical boundary conditions. Several plots of this type were computed to verify that the modified potential behaved appropriately, and these depict typical behavior.

## B. Initial Conditions

Monte Carlo techniques are used to determine the average collision characteristics for an ensemble of trajectories. For an ensemble of trajectories, we specify the translational temperature of the system in kelvins, the initial vibrational energy of  $H_2$ , the initial rotational energy of  $H_2$ , the initial vibrational energy of OH, the initial rotational energy of OH. All energies are expressed in kcal/mol. An ensemble is designated in the following manner:  $(T, v, J, v', J')$ , where  $T$  designates the translational temperature;  $v$ , the vibrational quantum number of  $H_2$ ;  $J$ , the rotational quantum number  $H_2$ ; with  $v'$  and  $J'$  defined analogously for OH.

The boundary conditions are selected in accord with the quasi-classical approximation and a Monte Carlo averaging scheme appropriate for a four atom, two molecule system.<sup>20</sup> The relative velocity for each trajectory is selected randomly by Monte Carlo sampling the appropriate collision integral with an assumed Boltzman distribution of velocities. The impact parameter  $b$  is selected from a  $b^2$  distribution of values between 0 and  $b_{\max}$ . The value of  $b_{\max} = 4.3$  bohr was selected by integrating a large number of trajectories with fixed values of the impact parameter. The reaction probability was found to be zero for trajectories with  $b > 4.3$  bohr. This was later verified by histogramming the trajectories, and the fraction of reactive trajectories in the last bin  $4.1 < b < 4.3$  was always zero or very small.

## C. Classical Trajectory Calculations

Hamilton's equations are used to describe the time evolution of the system. The eighteen equation of motion derived from this Hamiltonian are integrated using the ordinary differential equation solver ODE<sup>21</sup> written by Shampine and Gordon.<sup>22</sup> Solving the differential equation to a relative error of  $10^{-5}$  was found satisfactory for determining reaction cross section and pertinent energy transfer cross sections. Distance criteria were used to terminate the integration

and to determine whether or not reaction occurred.

Each trajectory could be divided into one of four classes: class A, no reaction; class B, reaction with the  $H_2$  atom included in the water molecule; class C, reaction with the  $H_3$  atom included in the water molecule; and class D, reaction with the  $H_2$  and  $H_3$  atoms included in the water molecule. For all trajectories, the time associated with integration of the trajectories, the scattering angle, and the final kinetic energy in the system was computed.

For non-reactive trajectories, the final energy of each molecule was determined and this was partitioned into vibrational and rotational energy using the following relationships:<sup>23</sup>

$$E_f^J = \min \left\{ V_D(r) + \frac{J_f^J \cdot J_f^J}{2\mu r^2} \right\} - V_D(r_e) \quad (2.6)$$

and

$$E_v = E_m^J - E_r^J \quad (2.7)$$

where  $E_f^J$  is the final rotational energy,  $V_D(r)$  is a Morse potential for the molecule in question,  $J_f^J$  is the final angular momentum for the molecule,  $r$  is the internuclear separation,  $\mu$  is the reduced mass,  $E_v^J$  is the final vibrational energy, and  $E_m^J$  is the final molecular internal energy. The minimum of the effective potential was found using the Newton-Raphson iteration technique. The final rotational quantum number  $J^J$  was determined from

$$J^J = -\frac{1}{2} + \frac{1}{2} [1 + 4J_f^J \cdot J_f^J / \hbar^2]^{\frac{1}{2}} \quad (2.8)$$

and the final diatomic vibrational quantum number,  $v^J$  was determined from

$$v^J = -\frac{1}{2} + \frac{1}{\pi\hbar} \int_{r_-}^{r_+} \left\{ 2\mu \left[ E_m^J - V_D(r) - \frac{J_f^J \cdot J_f^J}{2\mu r^2} \right] \right\}^{\frac{1}{2}} dr \quad (2.9)$$

where  $r_{\pm}$  are the turning points of the effective potential at the energy  $E_m^J$ .

For reactive trajectories, the final molecular energy,  $E_{H_2O}^J$ , the final molecular angular momentum  $J_{H_2O}^J$  and the angular momentum about the scattering

center  $J_g$  were determined. Energy was not partitioned within the water molecule since the potential does not treat the H atoms in water as identical. All energies are expressed in kcal/mol and all angular momenta are expressed as multiples of  $\hbar$ . Energy transfer characteristics will be discussed in a subsequent paper.

### III. REACTION CHARACTERISTICS

We have investigated reactivity in the  $H_2$ -OH system as a function of the initial translational temperature, vibrational energy of  $H_2$ , rotational energy of  $H_2$ , vibrational energy of OH, and rotational energy of OH. The range of translational temperatures investigated was between 300 and 4000 K, with emphasis placed upon 1200 and 2000 K. The initial value of the rotational quantum number was in the range 0-6 for  $H_2$ , and 0-7 for OH. The initial values of the vibrational quantum number for both molecules was varied between 0 and 4. Tables I through VII summarize the results of our study, and will be discussed, in turn, in the text. Each table uses the first five columns to identify a particular ensemble. The next column in the table, designated by the symbol TNT, is the number of trajectories computed for the ensemble, TNRT, is the total number of reactive trajectories, PR is the percent reactivity, and Q is the reaction cross section in bohr.<sup>2</sup> The statistical error for the various ensembles is approximately 10%, and is most generally less than 7%.

Some general trends were noted for the reactions. The number of class B and class C reactions were nearly identical. Each H from the  $H_2$  thus reacts to form water with equal probability as expected. This result is also a confirmation of correct phase space averaging. No class D reactions occurred i.e., the bond between the O and H was never broken. Average scattering angles for reactive trajectories were between 80 and 110, indicating that the retreating H atom leaves at right angles.

Prior to discussing the dependence of reactivity on the initial distribution of energy in this two molecule system, it is useful to recall the pertinent energies for this system. The barrier on the S-E surface is 6.1 kcal/mol, and the exoergicity is 15.1 kcal/mol. The vibrational adiabatic barrier is close to the barrier height, and is 5.9 kcal/mol. The zero point energy of  $H_2$  is 6.1 kcal/mol and for OH it is 5.2 kcal/mol.

### A. The Effect of Translational Temperature

The effect of relative translational temperature on reactivity is summarized in Table I and is illustrated in Fig. 4. Reactivity increases monotonically with translational temperature, and the sharpest increase occurs between 300 and 2000 K. The reaction cross section for (600, 1, 0, 0, 0) is 3.1 bohr<sup>2</sup> while it is 16.5 bohr<sup>2</sup> for (2000, 1, 0, 0, 0), yielding a factor of 5 increase for a factor of 3.3 temperature increase. A factor of only 1.2 is determined between 2000 and 4000 K. An average of the initial translational energy of the reactive trajectories was computed for several ensemble and compared to the average initial translational energy of the ensemble for temperatures of 1200 and 2000 K. In both cases, the average initial translational energy of the reactive trajectories was greater than the average initial translational energy; however the difference between the two averages was considerably greater at 1200 than 2000 K. At 2000 K, the molecules in the ensemble have, on the average, translational temperature to cross the barrier, and this is responsible for the leveling off of the reaction cross section vs translational temperature plot at 2000 K. It is not possible to directly compare our own results with those of Schatz<sup>7</sup> since our independent variables differ. Schatz found that the reaction cross section increases with translational energy, and his results indicate an abrupt increase, followed by a leveling off, in accord with our own results.

The influence of translational energy in enhancing reactivity is consistent with the character of an exoergic reaction. According to Hammond's postulate<sup>24</sup>

the transition state should be more similar to reactants than products since the reaction is exoergic. Walsh and Dunning<sup>3</sup> and Dunning et al.<sup>4</sup> found the saddle point to be in the entrance channel with the  $R_{OH}$  value, increased by 0.66 bohr in excess of the equilibrium value, and the  $R_{HH}$  separation incremented by 0.19 bohr. Mok and Polanyi<sup>25</sup> investigated the effect of barrier location on the reactions dynamics of the AB + CD system to determine the effects of different types of energy on reactivity. They found reagent translation to be more important than reagent vibrational energy in promoting reaction which has the barrier located in the entrance channel. This is in agreement with our own findings. The importance of translational energy in enhancing reactivity in the  $H_2 + OH$  system has been confirmed experimentally by Zeller and Steinert<sup>16</sup> who found that if the amount of energy corresponding to excitation of  $H_2$  from  $v = 0$  to  $v = 1$ , were instead put into relative translational energy of the reactants, a rate enhancement of  $5 \times 10^3$  would be observed. The rate of reaction of vibrationally excited  $H_2$  with OH was measured by them at 298 K.

### **B. The Effect of Rotational Energy**

The effect of reagent rotational energy on either or both molecules is summarized in Tables II, III, V, and VI. Tables II and V summarize the effect of reagent rotation for the cases where neither molecule is vibrationally excited, and are for 1200 and 2000 K, respectively. Rotational excitation of either or both  $H_2$  or OH suppresses reactivity. For cases when one and only one molecule has initial rotational energy, reactivity is suppressed in proportion to the rotational energy of that molecule. For example, the percentage suppression of reactivity resulting from increasing the initial rotational quantum number of  $H_2$  from  $J = 0$  to  $J = 4$  for  $H_2$ , corresponding to a gain of approximately 3 kcal/mol rotational energy, is about 55%. The percentage suppression is the same for rotationally exciting OH by the same amount of energy. This is illustrated in Figs. 5 and 6 where it is seen that the same percentage suppression occurs at both 1200 and 2000 K. Thus

there is no correlation between rotational suppression and translational temperature. If the rotational energy of one of the molecules is fixed, and the rotational energy of the other molecule is allowed to increase, reactivity is suppressed in proportion to the increasing rotational energy. The percentage decrease in reactivity is independent of the amount of fixed rotational energy of the other molecule, and it thus appears that the rotational motions of both molecules are uncorrelated. Tables III and VI summarize the effect of reagent rotation on reactivity when  $H_2$  is initially excited to  $v = 1$ , for 1200 and 2000 K, respectively. These effects are also illustrated in Figs. 5 and 6, where it is seen that the same behavior as that noted for the  $v = 0$  is observed. The percentage suppression is somewhat less when  $H_2$  is excited vibrationally, and the effects of two molecule rotational excitation is less regular than for the case when there is no initial vibrational excitation in the system.

Schatz<sup>7</sup> examined the effect of initial rotational excitation of OH and  $H_2$  on reactivity. He considered the case of separately increasing the rotational energy of either molecule at a fixed value of the translational energy with both molecules were in the  $v = 0$  vibrational state. He found that increasing the rotational energy of either molecule suppressed reactivity, but that the suppression determined for the rotational excitation of OH was less than for  $H_2$ . Our results differ from his with respect to the relative importance of  $H_2$  and OH.

Relative to the effects of translational and vibrational energy on reactivity, there have been relatively few systematic studies on the effects of rotational excitation. This is attributable to the small size of rotational quanta, lack of experimental data, and the fact that it is difficult to relate rotational effects to characteristics of the potential energy surface. Karplus et al.,<sup>26</sup> found that the J dependence of the reaction cross section was small for  $H+H_2$ , but their results indicate that plots expressing the reaction cross section as a function of translational energy become steeper as J increases, and that the threshold values tended to become larger with J. Muckerman<sup>27,28</sup> found that the cross section in-



creased between  $J = 0$  and  $1$  for  $F + H_2$  and then decreased with increasing  $J$ . He also found that the cross section decreased with  $J$  for  $F + HD$  and  $F + D_2$  and he reported an inversion of the intramolecular isotope effect with rotational excitation. For the  $F + HD$  reaction,  $DF$  is formed preferentially over  $HF$  for  $J = 0$  and  $1$ , while  $HF$  is the preferred product for  $J > 2$ . Jaffe and Anderson,<sup>29</sup> using a slightly different potential energy surface than Muckerman found the same dependence of reaction cross section on rotational excitation of  $H_2$  for the  $F + H_2$  system as Muckerman. Polanyi and Schreiber<sup>30</sup> also investigated the effect of reagent rotation on reactivity in the  $F + H_2$  system for several different potential energy surfaces. They explained the effect of reagent rotation by determining the ratio of the time spent in the approach coordinate to the time required for the rotation of the reactant molecule. If this ratio is large, a decrease in the cross section with  $J$  obtains, and if the ratio is small a modest increase in the cross section with  $J$  occurs. The Polanyi-Schreiber explanation is based upon the assumption of a linear transition state. It is important to note that wells along the approach coordinate increase the time of approach, thereby increasing the ratio, and should result in greater suppression of reactivity with increasing  $J$ . Blais and Truhlar<sup>31</sup> also noted an inversion of the dependence of reaction cross section with  $J$  for  $F + D_2$ , and report that their surface had a long range attractive well. They indicate that long range attractive forces play a role in determining the rotational dependence of reaction cross sections.

It is clear that rotational energy is not used to cross the reaction barrier in the  $H_2 + OH$  system since it inhibits reaction rather than promotes it. Examination of the energy transfer characteristics of the system revealed no significant transfer of energy from translation to rotation, which also would explain the suppression of reaction, since translational energy is so effective for crossing the barrier. The time spent along the approach coordinate is approximately  $10^{-13}$  sec. The  $H_2$  rotational period is  $2.7 \times 10^{-13}/J(J + 1)$  and  $OH$  rotates somewhat slower for a given  $J$ . There is time for a considerable amount of rotation for either molecule along the approach coordinate. Since the transition state is co-

planar and the molecules change their relative orientation several times during approach as a result of molecular rotation, we believe the major effect of rotation is to reduce the probability of achieving the proper  $H_2$ -OH orientation required for reaction. This is most easily seen for OH. The center of mass of the OH molecule is located very close to the O atom. As OH rotates, the H atom displacement vector sweeps out a much larger volume in coordinate space than the O atom in a given time interval. This greatly enhances the probability of the H atom being close to the incoming  $H_2$  molecule during approach and thus reduces the probability for reaction. The faster the OH is rotating, the less probable reaction becomes since the O has less chance of being in a favorable orientation for the incoming  $H_2$ . The situation with regard to  $H_2$  is less obvious, however, because the two atoms are identical. The difficulty of achieving the coplanar transition state increases with  $H_2$  rotational energy. If one refers to the arguments set forth by Polanyi and Schreiber, the ratio of the approach time to the rotation time, increases with  $H_2$  rotational energy. This would tend to increase the suppression of reaction by rotation. Although these arguments were posed for collinear transition states of atom-molecule reactions, they appear to have greater applicability. The suppression of reactivity by reagent rotation is also sensitive to the long range attractive forces of a potential energy surface. The major difference between our own surface and the Schatz-Elgersma surface is that the long range attractive forces have been removed from our surface. This has had an effect on the dependence of reaction cross section on reagent rotation. Schatz found less suppression by rotational excitation of OH and more suppression by  $H_2$  than we have. The effect of removing the long range attractive forces has been to reduce the suppression of reactivity by  $H_2$  rotation by decreasing the time required for approach.

### C. The Effect of Vibrational Energy

The effect of reagent vibrational excitation in either molecule or both molecules is summarized in Tables IV and VII for translational temperatures of 1200 and 2000 K, respectively. At 1200 K, after accounting for the statistical errors in the reaction cross sections, no change in reactivity occurs as a result of exciting  $H_2$  from  $v = 0$  to  $v = 1$ . Only a slight increase is noted for  $v \leq 3$ , and a more substantial increase is observed by exciting  $H_2$  to  $v = 4$ . Within statistical error, no change in reaction cross section is observed for exciting OH between  $v = 0$  and  $v = 2$ , and a slight decrease is noted for the higher vibrational excitation of OH to  $v = 3$  or 4. Exciting both molecules to  $v = 1$  yields the same reaction cross section as that determined for both molecules in  $v = 0$ . At a translational temperature of 2000 K, we see a monotonic increase in the reaction cross section with increasing vibrational excitation of  $H_2$ . Vibrational excitation of OH between  $v = 0$  and 4 produces a negligible change in the reaction cross section. Excitation of both molecules to  $v = 1$  yields the same cross section as observed for the  $v = 0$  case. These results are illustrated in Figs. 7 and 8 where the reaction cross section (with error bars) is plotted as a function of vibrational energy.

Schatz found a more dramatic increase of reactivity with vibrational excitation of  $H_2$  than we observed. It is somewhat difficult to directly compare our results with his since we determined reaction cross sections as a function of translational temperature while he used relative translational energy as a dependent variable. He found the effect of vibrationally exciting  $H_2$  to be more important for cases where the translational energy was insufficient to cross the barrier, and the enhancement factor decreased with increasing translational energy. At 1200 K, we noted that the average initial translational energy of the reacting molecules was greater than the average translational energy of the ensemble, and that this difference in the two averages decreased at 2000 K. Since translational energy is more effective for crossing the barrier due to barrier location, and sufficient amounts of translational energy are available in both the

1200 and 2000 K ensembles, it is used preferentially over vibrational energy, and we do not see a significant enhancement due to vibration. We concur with Schatz with regard to the effect of vibrational excitation of OH on reactivity.

The effects of reagent vibration on reactivity have been explained quite successfully by Schatz and Dunning et al., and will be briefly summarized here. One must assume a diabatic correlation between the OH stretching modes in reactant OH and in the transition state, and between the  $H_2$  stretching mode in the reactant and the transition state. At the transition state, the OH bond differs slightly from the reactant OH bond since there is only a small decrease in frequency ( $82 \text{ cm}^{-1}$ ) in going from reactant to the transition state. This bond acts as a spectator during the course of reaction, and does not contribute to crossing of the barrier. On the other hand, the  $H_2$  bond at the transition state is considerably different from the reactant  $H_2$  bond, and a decrease in frequency of  $2341 \text{ cm}^{-1}$  is observed in going from reactant to the transition state. This bond couples strongly with the reaction coordinate motion, and thus vibrational excitation of  $H_2$  influences reactivity. The greater influence of higher vibrational states in enhancing reactivity results from a greater amount of coupling, which is a result of the greater anharmonicity associated with the higher vibrational states.

#### IV. DETERMINATION OF THE THERMAL RATE COEFFICIENT

The reaction cross sections evaluated at 1200 and 2000 K were used to compute a thermal rate coefficient. The general expression for the thermal rate coefficient is:

$$k(T) = \frac{1}{2} \frac{1}{Q_v} \frac{1}{Q_J} \frac{1}{Q_{v'}} \frac{1}{Q_{J'}} \frac{1}{Q_{J'}} \sum_{\tau} \sum_{\mathcal{J}} \sum_{\tau'} \sum_{\mathcal{J}'} F_J(2J+1) F_{J'}(2J'+1) \times \exp(-E_{vJ}/kT) \exp(-E_{v'J'}/kT) k(v, J, v' J') \quad (4.1)$$

where

$$k(v, J, v', J') = N_0 \left( \frac{2\pi}{\pi} \right)^{3/2} \left( \frac{\mu}{kT} \right)^{3/2} Q(v, J, v', J', V_r) \cdot V_r^3 \exp(-V_r^2/2kT) \quad (4.2)$$

Choosing the relative translational velocity  $V_r$  according to a Boltzmann distribution enabled us to average over the Boltzmann distribution using Monte Carlo methods. The vibrational-rotational partition function for both molecules  $Q_v Q_J$  and  $Q_{v'} Q_{J'}$  were determined by assuming that the molecule was a harmonic oscillator-rigid rotator. The rotational partition function for  $H_2$  included treatment of identical particle symmetry. The factors  $F_J$  and  $F_{J'}$  are the nuclear spin degeneracy weighting factors. A factor of 1/2 has been included in Eq. (4.1) to account for the fact that only one half of the reagent  $H_2(^1\Sigma) + OH(^2\Pi)$  collisions sample the  $HHOH(^2A')$  reactive potential surface. The factor of 1/2 should be used to correct all reaction cross sections tabulated in the paper prior to comparing them with experimentally determined values. The values of the vibrational-rotational energies ( $E_{v,J}$  and  $E_{v',J'}$ ) required for the evaluation of the Boltzmann weighting factors were identical to input values used to determine the initial boundary conditions, and were evaluated from the values of  $D_e$ ,  $\beta$ , and  $r_e$  given by Schatz and Elgersma. Intermediate values of reaction cross sections were obtained through linear interpolation, and values of cross sections corresponding to larger values of J were determined by extrapolation. The quantity  $N_0$  is Avogadro's number.

In the calculation of the rate coefficient at 1200 K, the states of maximum rotational population are  $J = 3$  for  $H_2$ , and  $J = 4$  for OH. The  $v = 0$  state accounts for 99.4% of the vibrational population for  $H_2$  and 98.7% of the OH vibrational population. The  $H_2$  rotational states which made the greatest contribution to the rate coefficient were  $J = 1$  and 3, and those for OH were  $J = 3$  and 4. Cross sections determined by extrapolation were small, had small weighting factors, and thus made relatively small contributions to the thermal rate. The rate coefficient computed for 1200 K is determined largely from cross sections for both molecules in

the  $v = 0$  vibrational state (the 0-0 case). This is illustrated by Table VIII, where the contributions of various combinations of vibrational states to the thermal rate coefficient are listed. These are not state-to-state rate coefficients, but are instead the contributions that various states make to the thermal rate coefficient, i.e., the cross sections have been weighted by the appropriate Boltzmann factors. The thermal rate is dominated by the 0-0 case at 1200 K. The (1,0) cross sections make a contribution to the thermal rate coefficient which is two orders of magnitude less than the (0-0) case. One would expect the contribution from the (0-1) states to approximately equal to those from the (1-0) states, and contributions from the (1-1) case to be even less, since the statistical weight for both molecules vibrationally excited is very small.

In the evaluation of the thermal rate coefficient at 2000 K, the states of maximum rotational population are  $J = 3$  for  $H_2$  and  $J = 5$  for OH. The maximum contribution to the rate coefficient was from  $J = 1$  and 3 for  $H_2$  and from  $J = 3$  and 4 for OH. The  $v = 0$  state of  $H_2$  accounted for 95% of the vibrational population while it accounted for 93% of the vibrational population for OH. The contributions to the thermal rate coefficient made from cross sections associated with the following combinations of vibrational states: (0-0), (1,0), (0,1), and (1,1), are listed in Table VIII. Again it is seen that the (0-0) cross sections dominate the thermal rate, the (0-1) and (1-0) states make contributions that are an order of magnitude less, and the (1-1) state contribution is two orders of magnitude less. The rate coefficient for  $H_2$  in  $v = 0$  and OH in  $v = 1$  was estimated by assuming that the cross sections do not change when OH is excited from  $v = 0$  to 1. Addition of the contributions listed in Table VIII yields a thermal rate coefficient at 2000 K of

$$k = 1.8 \times 10^{13} \text{ cm}^3/\text{mol sec.} \quad (4.3)$$

Steiner<sup>17</sup> reports an extrapolated value for the rate coefficient of 2.1 and  $8.3 \times 10^{12} \text{ cm}^3/\text{mol sec}$ , at 1200 and 2000 K, respectively. Ravishankara et al.,<sup>13</sup> described their rate coefficient for  $H_2 + OH$ , measured between 250 and 1050 K, by a

three parameter function which can be used to evaluate the rate at higher temperatures. Extrapolation of their expression gives  $0.28$  and  $1.5 \times 10^{13} \text{ cm}^3/\text{mol sec}$  for  $1200$  and  $2000$  K, respectively. In their paper, they indicate a great deal of scatter obtains in plots of experimentally determined rate coefficients in the temperature regime between  $1000$  and  $2000$  K. The Arrhenius plot for the rate coefficient is decisively non-linear for temperatures above  $500$  K.

Our calculated rate coefficient compares favorably with experimentally determined values at  $2000$  K. The agreement at  $1200$  K is less satisfying. The calculated rate coefficient increases by a factor of  $2$  when the temperature is changed from  $1200$  to  $2000$  K, while experimentally determined values change by a factor of  $4$  or  $5$  over the same temperature interval. Our rate coefficient for  $1200$  K is clearly too large, and merits some discussion. At  $1200$  K the average translational energy in the system is  $3.6 \text{ kcal/mol}$  and is less than the barrier height. Although reacting molecules were found to have average translational energies in excess of the average for the ensemble, perhaps they also used a small amount of the zero point energy in crossing the barrier, thus producing cross sections which were too high. At  $2000$  K where the average translational energy was approximately equal to the barrier height, the agreement between calculated and experimental values is good. It is important to note that there was no bias involved in selecting the relative translational velocities according to the appropriate Boltzmann distribution. The velocities generated were histogrammed and found to produce the desired distribution. The analytical fit of the potential energy surface is particularly sensitive to the saddle point region where the density of *ab initio* points is high. The surface still may contain undesirable long range behavior which affects lower energy trajectories more those at higher energies, and this might result in erroneous, lower energy cross sections.

## V. SUMMARY AND CONCLUSIONS

We have performed classical trajectory calculations to determine the influence of translational temperature,  $H_2$  vibrational energy,  $H_2$  rotational energy, OH vibrational energy, and OH rotational energy on the reaction  $H_2 + OH \rightarrow H_2O + H$ . The Schatz-Elgersma analytical fit to the Walsh-Dunning surface was modified to remove spurious wells in the asymptotic region of the surface. In general reactivity is influenced by translational temperature,  $H_2$  vibrational energy, and reagent rotational energy. The most important effects can be summarized as follows:

1. The reaction cross section increases with translational temperature and is most strongly dependent upon it. This is in accord with previous results describing reactivity on surfaces with early barriers, and with experimental studies of the  $H_2 + OH$  reaction.

2. Rotational excitation of either or both reagent molecules suppresses reactivity in proportion to the rotational energy. There is no correlation between reactivity suppression by rotational energy and translational temperature, and the rotational motions of both molecules are uncorrelated. The major effect of reagent rotation is to reduce the probability of achieving the proper  $H_2 - OH$  orientation required for reaction.

3. Vibrational excitation of  $H_2$  has little effect upon reactivity for ensembles at 1200 K with vibrational states,  $v \leq 3$ . An increase in reactivity is observed at  $v =$

4. For ensembles at 2000 K a monotonic increase in reaction cross section occurs with increasing  $H_2$  vibrational energy. The motion associated with the  $H_2$  bond is coupled to the reaction coordinate motion, with the result that vibrational excitation influences reactivity.

4. Vibrational excitation of OH between  $v = 0$  and 4 produces a negligible change in the reaction cross section. The OH bond acts as a spectator during the reaction, and does not contribute energy to crossing the barrier.



A thermal rate coefficient was computed at 1200 and 2000 K. The computed value compares favorably with experimentally determined values at 2000 K. The agreement at 1200 K is less satisfactory since the computed value appears to be too large. The agreement between theory and experiment at both temperatures, however, indicates that the potential surface is a reasonable representation of the HHOH potential energy.

#### **ACKNOWLEDGMENTS**

This research was supported by the Director, Office of Energy, Office of Basic Energy Science, Chemical Sciences Division of the U.S. Department of Energy, under Contract No. DE-AC03-76SF00098.

## REFERENCES

- <sup>1</sup>N. J. Brown, K. H. Eberius, R. M. Fristrom, K. H. Hoyermann, and H. Gg. Wagner, *Combust. Flame* **33**, 151 (1978).
- <sup>2</sup>J. Warnatz, Sandia National Laboratories Report SAND83-8606, Livermore, CA (1983).
- <sup>3</sup>S. P. Walsh and T. H. Dunning, *J. Chem. Phys.* **72**, 1303 (1980).
- <sup>4</sup>T. H. Dunning, S. P. Walch, and A. F. Wagner, in *Potential Energy Surfaces and Dynamics Calculations*, edited by D. G. Truhlar (Plenum, New York, 1981), p. 329.
- <sup>5</sup>G. C. Schatz and H. Elgersma, *Chem. Phys. Lett.* **73**, 21 (1980).
- <sup>6</sup>G. C. Schatz and H. Elgersma in *Potential Energy Surface and Dynamics Calculations*, edited by D. G. Truhlar (Plenum, New York, 1981), p. 311.
- <sup>7</sup>G. C. Schatz, *J. Chem. Phys.* **74**, 1133 (1981).
- <sup>8</sup>G. C. Schatz and S. P. Walch, *J. Chem. Phys.* **72**, 776 (1980).
- <sup>9</sup>A. D. Isaacson and D. G. Truhlar, *J. Chem. Phys.* **76**, 1380, (1982).
- <sup>10</sup>N. J. Brown and A. S. Edlin, Transition State Calculations of the Thermal Rate of the  $H_2 + OH \rightarrow H_2O + H$  Reaction Including Isotope Effects, Tunneling and Angular Momentum Conservation. (To be published).
- <sup>11</sup>D. L. Baulch, D. D. Drysdale, D. G. Horne and A. C. Lloyd, *Evaluated Kinetic Data for High Temperature Reactions*, **2**, (Butterworths, London, 1972).
- <sup>12</sup>G. Dixon Lewis and D. J. Williams in *Comprehensive Chemical Kinetics* **17**, edited by C. H. Bainford and C. F. H Tipper (Elsevier Scientific Publishing Company, Amsterdam, the Netherlands, 1977), p. 1.
- <sup>13</sup>A. R. Ravishankara, J. M. Nicovich, R. L. Thompson, and F. P. Tully, *J. Phys. Chem.* **85**, 2498 (1981).
- <sup>14</sup>J. E. Spencer, H. Endo and G. P. Glass, 16th Symposium (Int) on Combustion (The Combustion Institute, Pittsburgh, PA), 829 (1976).
- <sup>15</sup>G. C. Light and J. H. Matsumoto, *Chem. Phys. Lett.* **58**, 578 (1978).
- <sup>16</sup>R. Zellner and W. Steinert, *Chem. Phys. Lett.* **81**, 568 (1981).
- <sup>17</sup>W. Steinert, Ph.D. Thesis, University of Gottingen (1979).
- <sup>18</sup>K. S. Sorbie and J. N. Murrell, *Mol. Phys.* **29**, 1387 (1975).
- <sup>19</sup>R. J. Bartlett, I. Shavitt and G. D. Purves, *J. Chem. Phys.* **71**, 281 (1979).
- <sup>20</sup>N. J. Brown and D. M. Silver, *J. Chem. Phys.* **65**, 311 (1976).
- <sup>21</sup>T. H. Jefferson, Sandia National Laboratories Report SAND77-8274, Livermore, CA (1977).

- <sup>22</sup>L. F. Shampine and M. K. Gordon, *Computer Solutions of Ordinary Differential Equations: The Initial Value Problem* (Freeman, San Francisco, 1975).
- <sup>23</sup>D. G. Truhlar and J. T. Muckerman, in *Atom-Molecule Collision Theory, A Guide for Experimentalist*, edited by R. B. Bernstein (Plenum Press, New York, 1979), p. 505.
- <sup>24</sup>G. S. Hammond, *J. Am. Chem. Soc.* **77**, 334 (1955).
- <sup>25</sup>M. H. Mok and J. C. Polanyi, *J. Chem. Phys.* **53**, 4588 (1970).
- <sup>26</sup>M. Karplus, R. N. Porter, and R. D. Sharma, *J. Chem. Phys.* **43**, 3259 (1956).
- <sup>27</sup>J. T. Muckerman, *J. Chem. Phys.* **54**, 1155 (1971).
- <sup>28</sup>J. T. Muckerman, *J. Chem. Phys.* **56**, 2997 (1972).
- <sup>29</sup>R. L. Jaffe, and J. B. Anderson, *J. Chem. Phys.* **54**, 2224 (1971).
- <sup>30</sup>J. C. Polanyi, and J. L. Schreiber, *Faraday Discuss. Chem. Soc.* **62**, 267 (1977).
- <sup>31</sup>N. C. Blais, and D. G. Truhlar, *J. Chem. Phys.* **58**, 1090 (1973).

## LIST OF TABLES

- I. Summary of reactivity for various ensembles of differing translational energy. Symbols are defined in text. The units of translational temperature are Kelvins and those for reaction cross section are square bohrs.
- II. Summary of reactivity for various ensembles at 1200 K, with  $\nu_{H_2} = 0$  and  $\nu_{OH} = 0$ , differing in the amount of initial rotational energy in the reactant molecules. The units of reaction cross section are square bohrs.
- III. Summary of reactivity for various ensembles at 1200 K, with  $\nu_{H_2} = 1$  and  $\nu_{OH} = 0$ , differing in the amount of initial rotational energy in the reactant molecules. The units of the reaction cross section are square bohrs.
- IV. Summary of reactivity for various ensembles at 1200 K, with  $j_{H_2} = 0$  and  $j_{OH} = 0$ , differing in the amount of initial vibrational energy in the reactant molecules. The units of the reaction cross section are square bohrs.
- V. Summary of reactivity for various ensembles at 2000 K, with  $\nu_{H_2} = 0$  and  $\nu_{OH} = 0$ , differing in the amount of initial rotational energy in the reactant molecules. The units of the reaction cross section are in square bohrs.
- VI. Summary of reactivity for various ensembles at 2000 K, with  $\nu_{H_2} = 1$  and  $\nu_{OH} = 0$ , differing in the amount of initial rotational energy in the reactant molecules. The units of reaction cross section are square bohrs.
- VII. Summary of reactivity for various ensembles at 2000 K, with  $j_{H_2} = 0$  and  $j_{OH} = 0$ , differing in the amount of initial vibrational energy in the reactant molecules. The units of reaction cross section are square bohrs.
- VIII. Contributions from various vibrational states to the thermal rate coefficient,  $k_p(T)$ , at 1200 and 2000 K. The units of temperatures are in Kelvins and those for the partial rate coefficients are  $cm^3/mol \cdot sec$

TABLE I								
$T^a$	$\nu_{H_2}^b$	$J_{H_2}^c$	$\nu_{OH}^d$	$J_{OH}^e$	TNT <sup>f</sup>	TNRT <sup>g</sup>	PR <sup>h</sup>	Q <sup>i</sup>
300	1	0	0	0	692	4		
600	1	0	0	0	2250	119	5.3%	3.1
800	1	0	0	0	1638	171	10.4	6.0
900	1	0	0	0	1687	201	11.9	6.9
1000	1	0	0	0	1297	197	15.2	8.8
1200	1	0	0	0	1033	201	19.5	11.3
1500	1	0	0	0	817	201	24.6	14.3
1700	1	0	0	0	745	201	27.0	15.7
1900	1	0	0	0	992	308	31.0	18.0
2000	1	0	0	0	1418	402	28.4	16.5
2200	1	0	0	0	631	201	31.9	18.5
2400	1	0	0	0	1495	486	32.5	18.9
3000	1	0	0	0	600	208	34.7	20.1
4000	1	0	0	0	600	212	35.3	20.5

a) Translation temperature in Kelvins

b)  $H_2$  vibrational quantum number

c)  $H_2$  rotational quantum number

d) OH vibrational quantum number

e) OH rotational quantum number

f) Total number of trajectories

g) Total number reactive trajectories

h) Percent reactivity

i) Q is reaction cross section in (bohr)<sup>2</sup>

TABLE II								
$T^a$	$v_{H_2}$	$J_{H_2}$	$v_{OH}$	$J_{OH}$	TNT	TNRT	PR	Q
1200	0	0	0	0	1166	201	17.2%	10.0
	0	1	0	0	3050	299	9.8	5.7
	0	2	0	0	2022	201	9.9	5.8
	0	3	0	0	2331	195	8.4	4.9
	0	4	0	0	2586	191	7.4	4.3
	0	6	0	0	3141	208	6.6	3.8
	0	0	0	0	1166	201	17.2%	10.0
	0	0	0	2	1426	201	14.1	8.2
	0	0	0	3	758	94	12.4	7.2
	0	0	0	4	1836	204	11.1	6.4
	0	0	0	5	2072	201	9.7	5.6
	0	0	0	7	3014	239	7.9	4.6
	0	2	0	0	2022	201	9.9%	5.8
	0	2	0	2	2369	190	8.0	4.7
	0	2	0	4	2459	201	8.2	4.7
	0	2	0	5	3419	201	5.9	3.4
	0	2	0	7	4093	187	4.6	2.6
	0	4	0	0	2586	191	7.4%	4.3
	0	4	0	2	3108	184	5.9	3.4
	0	4	0	4	4089	198	4.8	2.8
	0	4	0	5	6281	207	3.3	1.9
	0	4	0	7	5472	173	3.2	1.8
	0	0	0	4	1836	204	11.1%	6.4
	0	1	0	4	2999	246	8.2	4.8
	0	2	0	4	2459	201	8.2	4.8
	0	3	0	4	3712	201	5.4	3.1
	0	4	0	4	4089	198	4.8	2.8
	0	0	0	7	3014	239	7.9%	4.6
	0	1	0	7	2325	112	4.8	2.8
	0	2	0	7	4093	187	4.6	2.6
	0	3	0	7	5431	184	3.4	2.0
	0	4	0	7	5472	173	3.2	1.8

a) Notation defined in Table I

TABLE III								
$T^a$	$v_{H_2}$	$J_{H_2}$	$v_{OH}$	$J_{OH}$	TNT	TNRT	PR	Q
1200	1	0	0	0	1033	201	19.5%	11.3
	1	1	0	0	772	144	18.7	10.8
	1	2	0	0	1266	202	16.0	9.3
	1	3	0	0	727	113	15.5	9.0
	1	4	0	0	1460	194	13.3	7.7
	1	6	0	0	760	107	14.1	8.2
	1	0	0	0	1033	201	19.5%	11.3
	1	0	0	2	736	129	17.5	10.2
	1	0	0	4	1340	202	15.0	8.8
	1	0	0	5	731	99	13.4	7.8
	1	0	0	7	1370	184	13.4	7.8
	1	2	0	0	1266	202	16.0%	9.3
	1	2	0	2	2242	348	15.5	9.0
	1	2	0	4	1620	201	12.4	7.2
	1	2	0	5	2195	238	10.8	6.3
	1	2	0	7	2196	168	7.7	4.4
	1	4	0	0	1460	194	13.3%	7.7
	1	4	0	2	752	107	14.2	8.3
	1	4	0	4	1959	201	10.3	6.0
	1	4	0	5	4365	389	8.9	5.2
	1	4	0	7	2888	177	6.1	3.5
	1	0	0	4	1340	202	15.1%	8.8
	1	1	0	4	2179	267	12.3	7.1
	1	2	0	4	1620	201	12.4	7.2
	1	3	0	4	1455	170	11.7	6.8
	1	4	0	4	1959	201	10.3	6.0
	1	0	0	7	1370	184	13.4%	7.8
	1	1	0	7	2191	215	9.8	5.7
	1	2	0	7	2196	168	7.7	4.4
	1	3	0	7	2679	217	7.5	4.4
	1	4	0	7	2888	177	6.1	3.5

a) Notation defined in Table I

TABLE IV								
$T^a$	$\nu_{H_2}$	$J_{H_2}$	$\nu_{OH}$	$J_{OH}$	TNT	TNRT	PR	Q
1200	0	0	0	0	1166	201	17.2%	10.0
	1	0	0	0	1033	201	19.5	11.3
	2	0	0	0	813	169	20.7	12.0
	3	0	0	0	757	162	21.4	12.4
	4	0	0	0	751	200	26.5	15.4
	0	0	0	0	1166	201	17.2%	10.0
	0	0	1	0	1277	196	15.3	8.9
	0	0	2	0	728	118	16.2	9.4
	0	0	3	0	698	96	13.8	8.0
	0	0	4	0	692	92	13.3	7.6
	1	0	0	0	1033	201	19.5%	11.3
	1	0	1	0	1090	201	18.4	10.7
	0	0	1	0	1277	196	15.3	8.9

a) Notation defined in Table I



TABLE V								
$T^a$	$\nu_{H_2}$	$J_{H_2}$	$\nu_{OH}$	$J_{OH}$	TNT	TNRT	PR	Q
2000	0	0	0	0	864	202	23.4%	13.6
	0	1	0	0	1053	201	19.8	11.5
	0	2	0	0	1415	202	14.3	8.3
	0	3	0	0	1526	202	13.2	7.7
	0	4	0	0	1675	201	12.0	7.0
	0	6	0	0	1571	188	11.9	6.9
	0	0	0	0	864	202	23.4%	13.6
	0	0	0	2	802	176	21.9	12.7
	0	0	0	4	1151	201	17.5	10.2
	0	0	0	5	2213	320	14.5	8.4
	0	0	0	7	1692	202	11.9	6.9
	0	2	0	0	1415	202	14.3%	8.3
	0	2	0	2	1473	201	13.6	7.9
	0	2	0	4	1506	203	13.5	7.8
	0	2	0	5	2192	201	9.2	5.3
	0	2	0	7	2972	201	6.8	4.0
	0	4	0	0	1675	201	12.0%	7.0
	0	4	0	2	2248	234	10.5	6.1
	0	4	0	4	2366	201	8.5	4.9
	0	4	0	5	2993	233	7.8	4.5
	0	4	0	7	3028	199	6.6	3.8
	0	0	0	4	1151	201	17.5%	10.2
	0	1	0	4	1485	230	15.5	9.0
	0	2	0	4	1506	203	13.5	7.8
	0	3	0	4	2265	218	9.6	5.6
	0	4	0	4	2366	201	8.5	4.9
	0	0	0	7	1692	202	11.9%	6.9
	0	1	0	7	2205	193	8.8	5.1
	0	2	0	7	2972	201	6.8	4.0
	0	3	0	7	3050	215	7.1	4.1
	0	4	0	7	3028	199	6.6	3.8

a) Notation defined in Table I

TABLE VI								
$T^a$	$\nu_{H_2}$	$J_{H_2}$	$\nu_{OH}$	$J_{OH}$	TNT	TNRT	PR	Q
2000	1	0	0	0	1418	402	28.4%	16.5
	1	1	0	0	708	201	28.4	16.5
	1	2	0	0	741	192	25.9	15.0
	1	3	0	0	741	176	23.8	13.8
	1	4	0	0	755	161	21.3	12.4
	1	6	0	0	738	180	24.4	14.2
	1	0	0	0	1418	402	28.4%	16.5
	1	0	0	2	670	201	30.0	17.4
	1	0	0	4	732	180	24.6	14.3
	1	0	0	5	717	128	17.9	10.4
	1	0	0	7	725	137	18.9	11.0
	1	2	0	0	741	192	25.9%	15.0
	1	2	0	2	1469	356	24.2	14.1
	1	2	0	4	727	150	20.6	12.0
	1	2	0	5	1426	271	19.0	11.0
	1	2	0	7	723	95	13.1	7.6
	1	4	0	0	755	161	21.3%	12.4
	1	4	0	2	1467	320	21.8	12.7
	1	4	0	4	735	129	17.6	10.2
	1	4	0	5	2162	348	16.1	9.4
	1	4	0	7	721	104	14.4	8.4
	1	0	0	4	732	180	24.6%	14.3
	1	1	0	4	1442	318	22.1	12.8
	1	2	0	4	727	150	20.6	12.0
	1	3	0	4	1441	299	20.8	12.1
	1	4	0	4	735	129	17.6	10.2
	1	0	0	7	725	137	18.9%	11.0
	1	1	0	7	1407	264	18.8	10.9
	1	2	0	7	723	95	13.1	7.6
	1	3	0	7	1434	201	14.0	8.1
	1	4	0	7	721	104	14.4	8.4

a) Notation defined in Table I

TABLE VII								
$T^a$	$\nu_{H_2}$	$J_{H_2}$	$\nu_{OH}$	$J_{OH}$	TNT	TNRT	PR	Q
2000	0	0	0	0	864	202	23.4%	13.6
	1	0	0	0	1418	402	28.4	16.5
	2	0	0	0	500	173	34.6	20.1
	3	0	0	0	554	201	36.3	21.1
	4	0	0	0	496	201	40.5	23.5
	0	0	0	0	864	202	23.4%	13.6
	0	0	1	0	772	201	26.0	15.1
	0	0	2	0	701	136	19.4	11.3
	0	0	3	0	718	147	20.5	11.9
	0	0	4	0	673	144	21.4	12.4
	1	0	0	0	1418	402	28.4%	16.5
	1	0	1	0	1887	553	29.3	17.0
	0	0	1	0	772	201	26.0	15.1

a) Notation defined in Table I

TABLE VIII			
T	$\nu_{H_2}$	$\nu_{OH}$	$k_p(T)^a$
1200	0	0	$9.4 \times 10^{12}$
1200	1	0	$1.6 \times 10^{11}$
2000	0	0	$1.5 \times 10^{13}$
2000	1	0	$1.8 \times 10^{12}$
2000	0	1	$1.3 \times 10^{12}$
2000	1	1	$1.6 \times 10^{11}$

(a) Partial contribution to thermal rate. Units are  $cm^3 mol \cdot sec$

## LIST OF FIGURES

1. Schematic diagram defining the interatomic coordinates  $R_2$  through  $R_6$ .
2. Plots of S-E potential energy as a function of the intermolecular center of mass separation. The units of the potential energy are hartrees and those for the center of mass separation are bohrs.
3. Plots of R-B potential energy as a function of the intermolecular center of mass separation. The units of the potential energy are hartrees and those for the intermolecular center of mass separation are bohrs.
4. Plot of the reaction cross section as a function of translational temperature. The units of translational temperatures are Kelvins and those for the reaction cross section are square bohrs.
5. Plots of the reaction cross section as a function of the rotational energy for ensembles at 1200 K. The units of the reaction cross section are square bohrs and those for rotational energy are kcal/mol.
6. Plots of the reaction cross section as a function of the rotational energy for ensembles at 2000 K. The units of the reaction cross section are square bohrs and those for rotational energy are in kcal/mol.
7. Plots of the reaction cross section as a function of the vibrational energy for ensembles at 1200 K with  $j_{H_2} = 0$  and  $j_{OH} = 0$ . The reaction cross sections are square bohrs and those for the vibrational energy are kcal/mol.
8. Plots of the reaction cross section as a function of the vibrational energy for ensembles at 2000 K with  $j_{H_2} = 0$  and  $j_{OH} = 0$ . The units of the reaction cross sections are square bohrs and those for vibrational energy are kcal/mol.

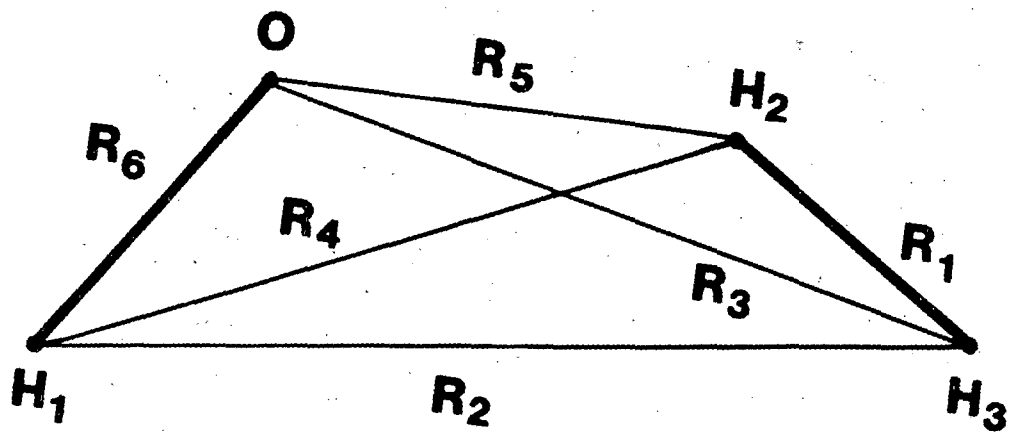


FIG.1

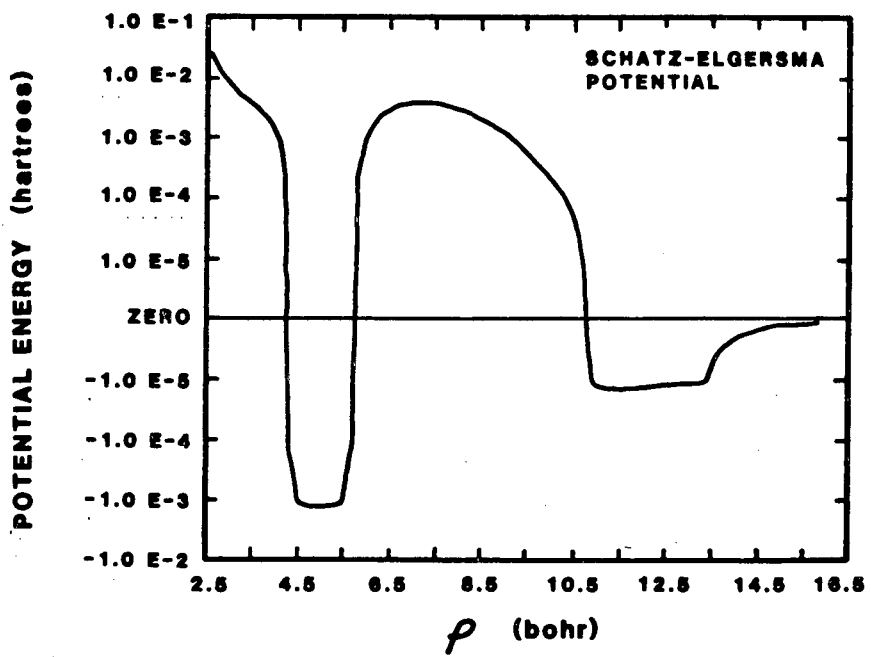
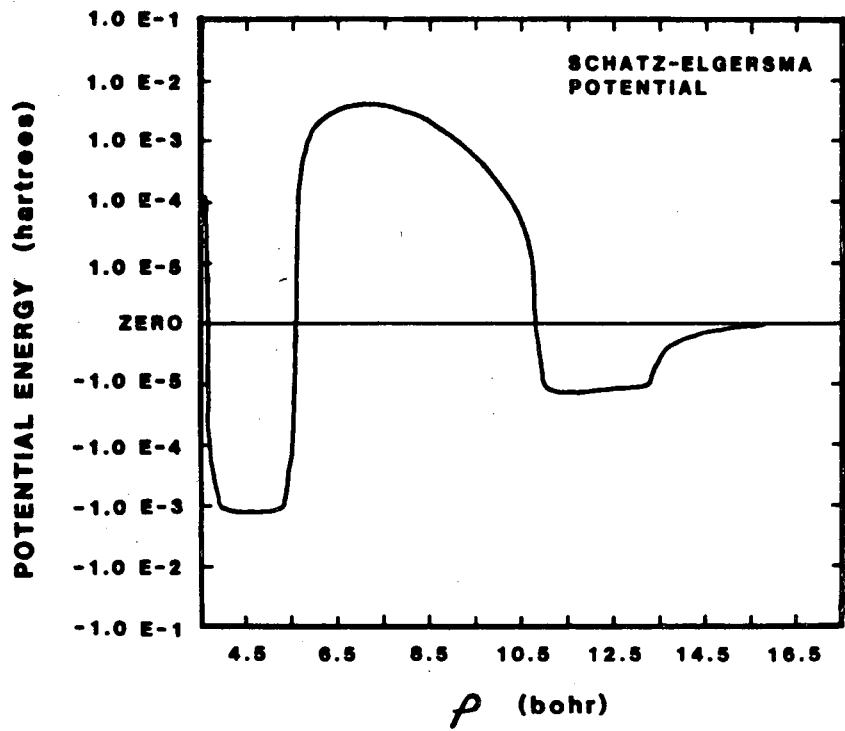


FIG. 2

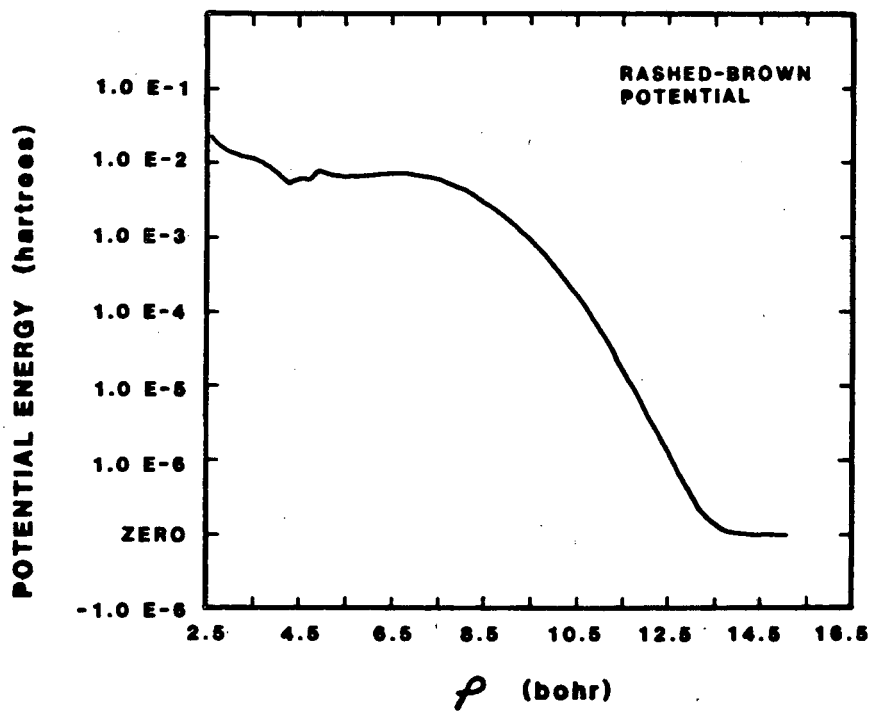
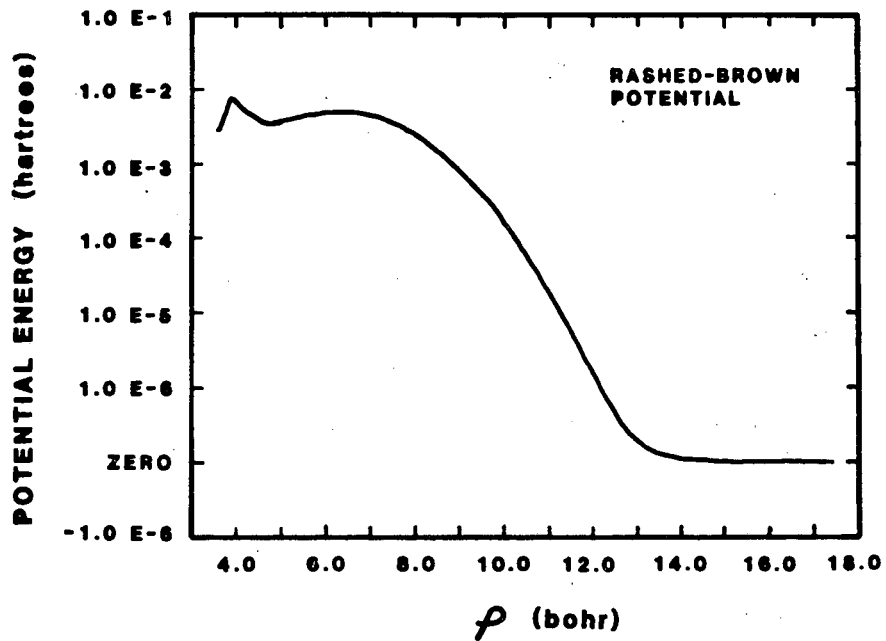


FIG. 3



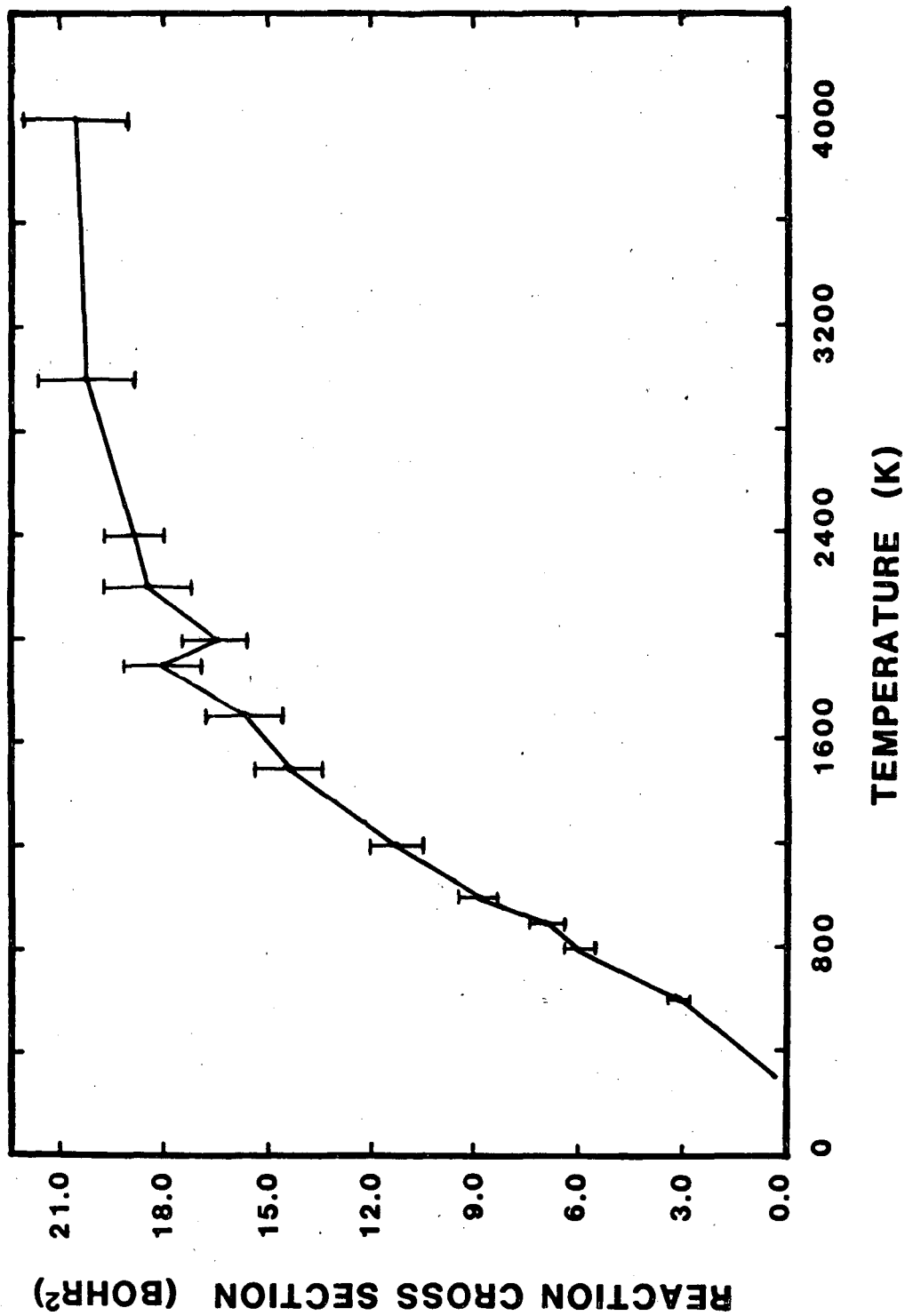


FIG.4

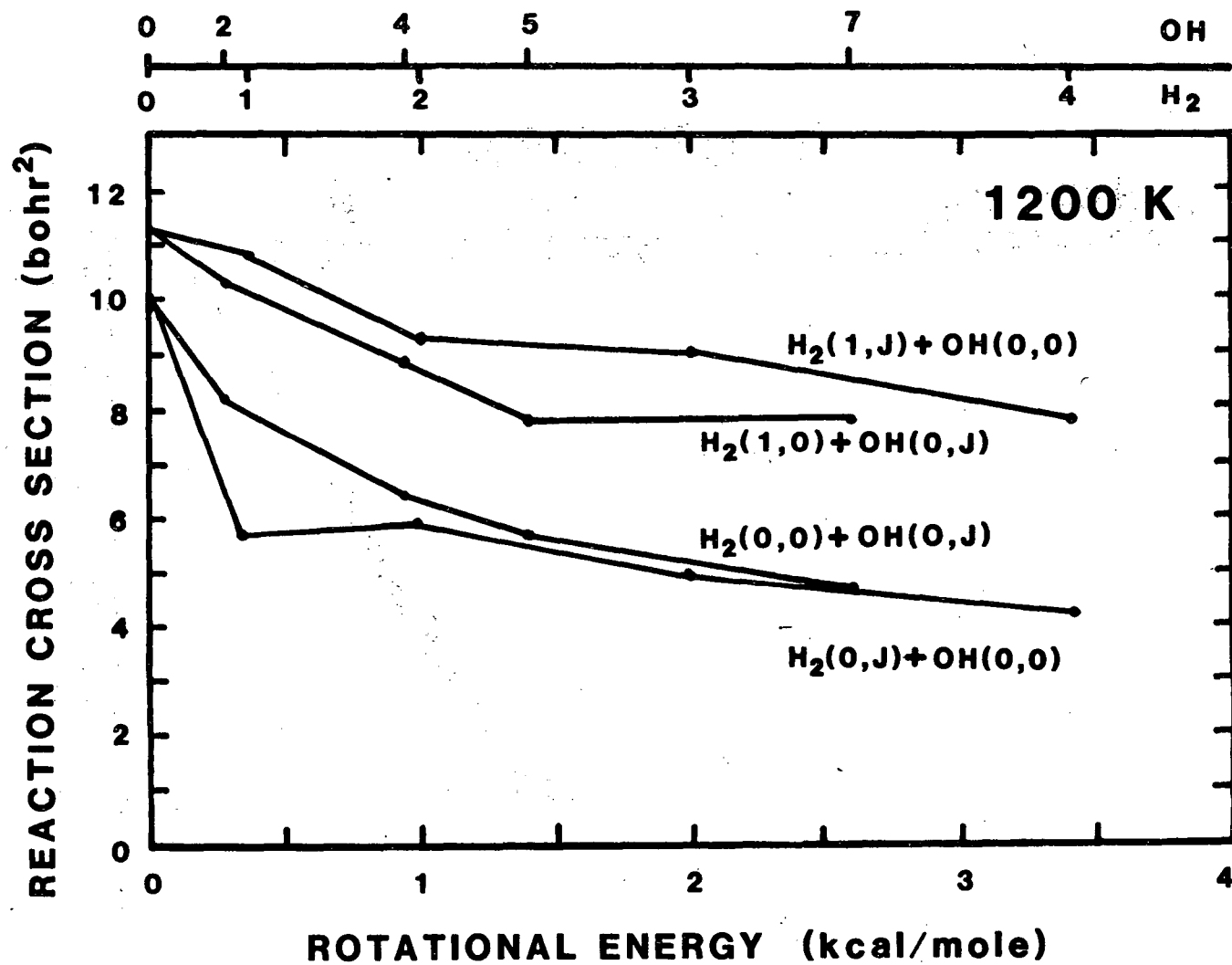


FIG.5

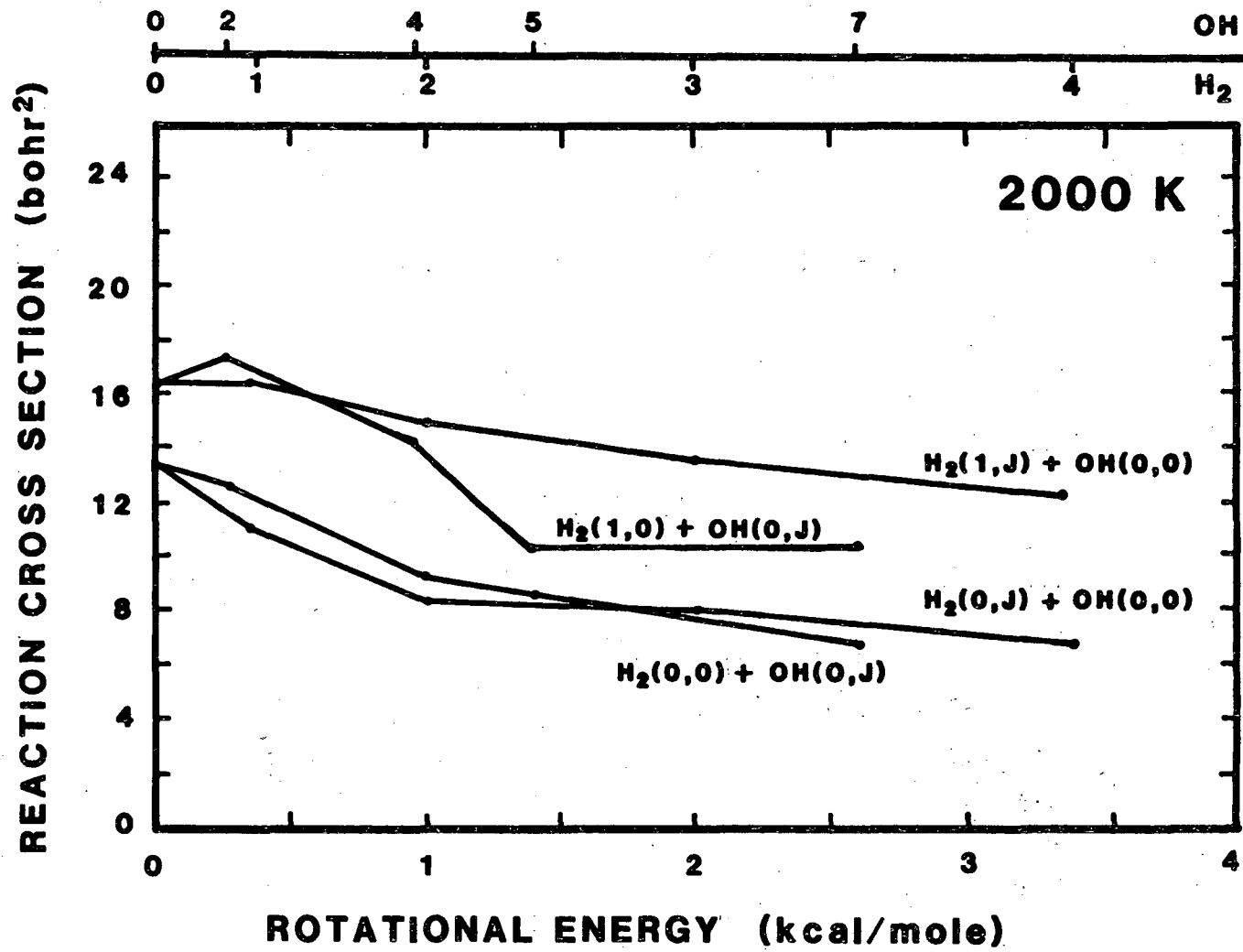


FIG.6

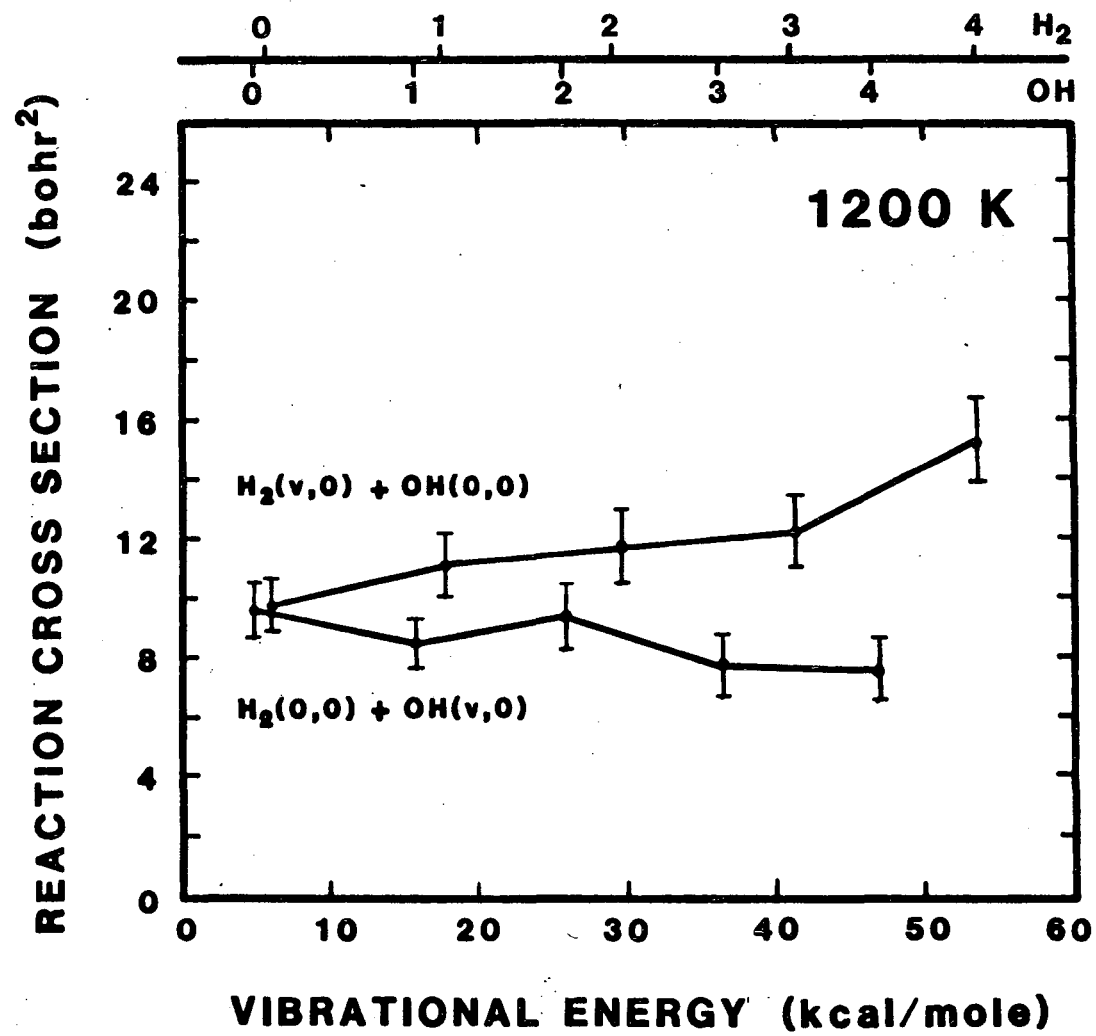


FIG.7

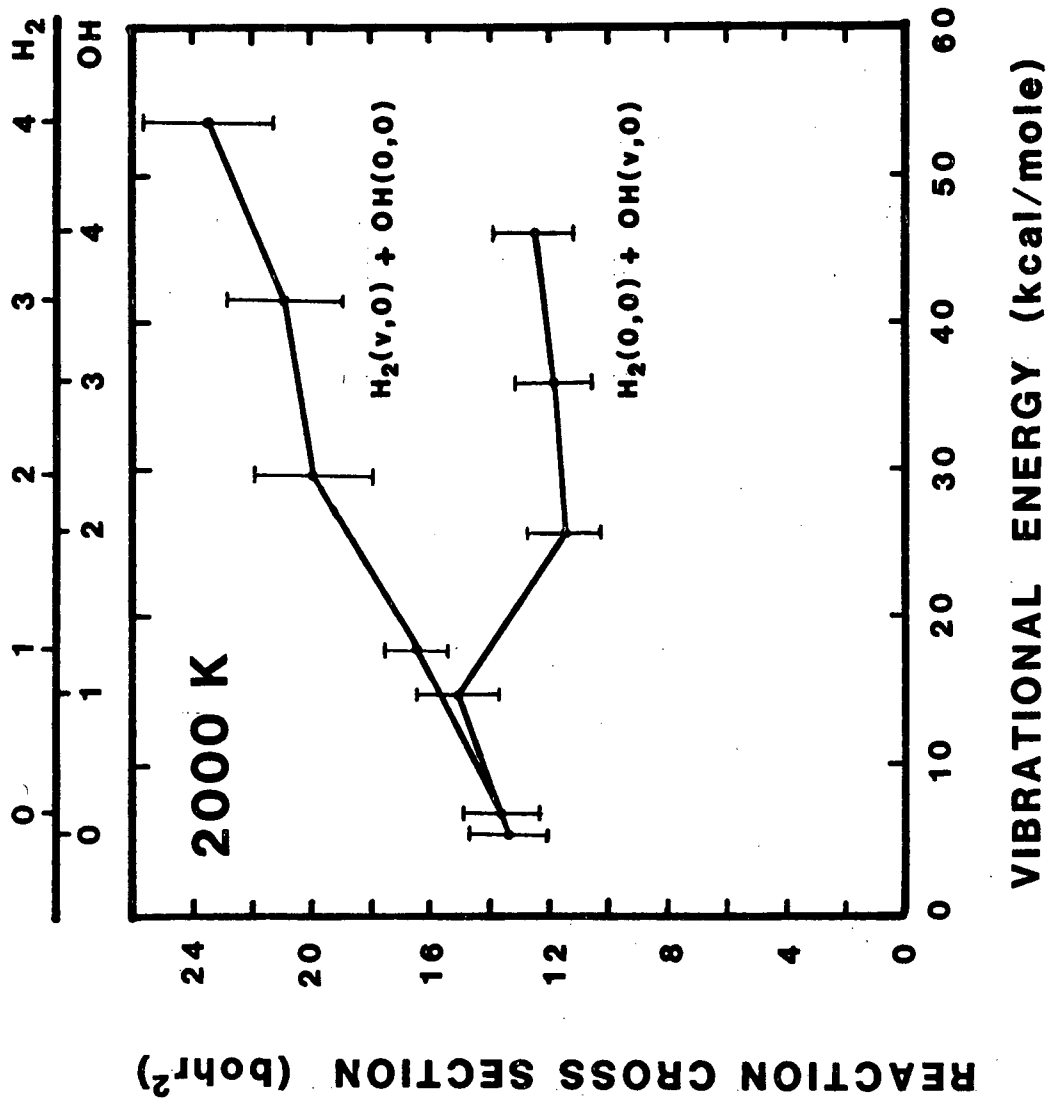


FIG.8

This report was done with support from the Department of Energy. Any conclusions or opinions expressed in this report represent solely those of the author(s) and not necessarily those of The Regents of the University of California, the Lawrence Berkeley Laboratory or the Department of Energy.

Reference to a company or product name does not imply approval or recommendation of the product by the University of California or the U.S. Department of Energy to the exclusion of others that may be suitable.

TECHNICAL INFORMATION DEPARTMENT  
LAWRENCE BERKELEY LABORATORY  
UNIVERSITY OF CALIFORNIA  
BERKELEY, CALIFORNIA 94720